Linear thermal expansion measurements of lead magnesium niobate (PMN) electroceramic material for the Terrestrial Planet Finder Coronagraph

Paul B. Karlmann*, Kerry J. Klein, Peter G. Halverson, Robert D. Peters,
Marie B. Levine, David Van Buren, Matthew J. Dudik
Jet Propulsion Laboratory, California Institute of Technology
4800 Oak Grove Drive, Pasadena, CA 91109-8099

ABSTRACT

Linear thermal expansion measurements of nine samples of Lead Magnesium Niobate (PMN) electroceramic material were recently performed in support of NASA's Terrestrial Planet Finder Coronagraph (TPF-C) mission. The TPF-C mission is a visible light coronagraph designed to look at roughly 50 stars pre-selected as good candidates for possessing earth-like planets. Upon detection of an earth-like planet, TPF-C will analyze the visible-light signature of the planet's atmosphere for specific spectroscopic indicators that life may exist there. With this focus, the project's primary interest in PMN material is for use as a solid-state actuator for deformable mirrors or compensating optics. The nine test samples were machined from three distinct boules of PMN ceramic manufactured by Xinetics Inc. Thermal expansion measurements were performed in 2005 at NASA Jet Propulsion Laboratory (JPL) in their Cryogenic Dilatometer Facility. All measurements were performed in vacuum with sample temperature actively controlled over the range of 270K to 310K. Expansion and contraction of the test samples with temperature was measured using a JPL-developed interferometric system capable of sub-nanometer accuracy. Presented in this paper is a discussion of the sample configuration, test facilities, test method, data analysis, test results, and future plans.

Keywords: PMN, CTE, thermal expansion, dilatometer, TPF, thermal strain

1. INTRODUCTION

The JPL Cryogenic Dilatometer Facility is designed to provide ultra-high precision measurements of thermal strain, dimensional stability and material hysteresis to support NASA's next generation of astronomical missions. Primary support for the development and operation of the facility is provided by the James Webb Space Telescope (JWST) Project. Additional support is provided by the Terrestrial Planet Finder Coronagraph (TPF-C) as well as the Space Interferometry Mission (SIM).

Recently, in support of the TPF-C project, nine test samples of Lead Magnesium Niobate (PMN) electroceramic material were fabricated and a subset tested in the JPL Cryogenic Dilatometer Facility. The TPF-C mission is a visible light coronagraph designed to examine 50 pre-selected stars with the potential of possessing earth-like planets. Upon detection of an earth-like planet, TPF-C will analyze the visible-light signature of the planet's atmosphere for specific spectroscopic life-indicators. With this focus, the project's primary interest in PMN material is for use as a solid-state actuator for deformable mirrors or compensating optics. Precise knowledge of this material's coefficient of thermal expansion (CTE) over the operating temperatures of interest will enable the optomechanical design and analysis of thermal-induced deformations and stresses within the deformable mirror and/or compensating optic.

2. APPARATUS

The basic design of the JPL Cryogenic Dilatometer has been previously described by Dudik et al.[1] with subsequent improvements and modifications to the system detailed by Karlmann et al.[2] The primary elements of the system are the laser source, interferometer, vacuum chamber, thermal control system, test sample alignment stage, signal processing electronics, and data acquisition and control system. Both the laser source and the interferometer are similar to those described by Zhao et al.[3,4] Shown in Figures 1, 2 and 3 are photos of the Cryo-Dilatometer Facility.

Optical Materials and Structures Technologies II, edited by William A. Goodman,
Proceedings of SPIE Vol. 5868 (SPIE, Bellingham, WA, 2005)
0277-786X/05/$15 · doi: 10.1117/12.615173

Figure 1. Laser source and vacuum chamber.

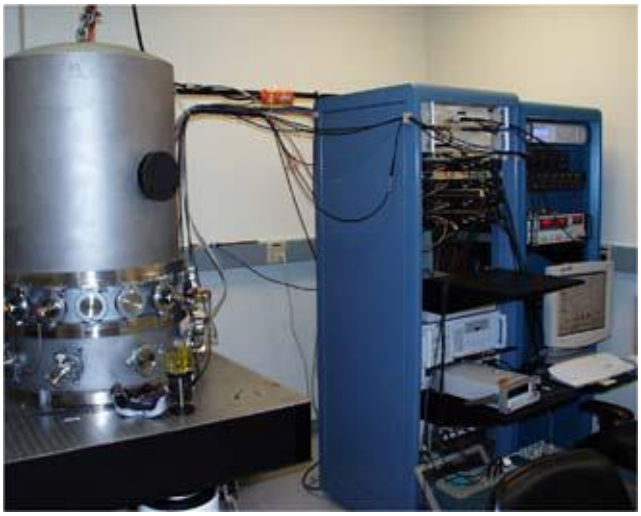
Figure 2. Vacuum chamber and electronics rack.

2.1 Laser source

The laser source is a 100mW, 532nm, temperature stabilized, doubled YAG laser. Output from the laser is split into a measurement beam at 80.016 MHz and a local oscillator beam at 80.000 MHz using acousto-optic modulators (AOMs). Both beams, separated by their 16 kHz heterodyne beat, are then sent via angle-polished optical fibers from the optical table via a feed-through into the vacuum chamber.

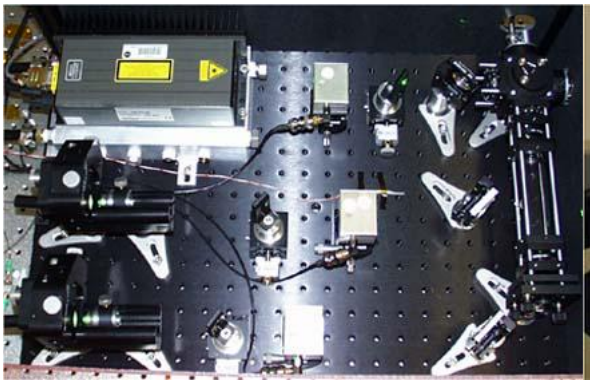
Figure 3. Laser source layout.


Figure 4. Interferometer center section.

2.2 Interferometer

Inside the vacuum chamber is a custom interferometer consisting of two off-axis parabolic mirrors (OAPs), two beam splitters, two fiber couplers, two beam masks and a photo-detector board. All of the components are held with kinematic flexural Invar 36 alignment mounts, and the basic structure is a monolithic piece of Invar 36 heat-treated for dimensional stability and supported by spring-loaded Zerodur bipods.

2.3 Vacuum chamber & thermal control system

The vacuum chamber is a ~0.8m dia. x 1m tall stainless steel vacuum belljar maintained at pressures below 5 x 10^{-5} torr by a turbo molecular pump backed by an oil-free scroll pump. A closed cycle helium cryocooler with vibration isolation is used to conductively cool a flexible thermal strap attached to the test sample thermal shroud. A pair of film heaters, silicon diode temperature sensors, and a Lakeshore 340 Temperature Controller are used for controlling the temperature of the test sample thermal shroud.

2.4 Test sample alignment stage

The test sample alignment stage uses PZT actuators and Invar screws with spherical nuts to provide the fine and course levels of tip-tilt adjustment necessary to maintain alignment between the reflecting surfaces of the test sample and the measurement beams of the interferometer. Coarse adjustment using the Invar screws and nuts acting on integral flexures provides 23 milliradians with a resolution of better than 13 microradians. Fine adjustment using the PZT actuators acting on integral flexures provides 220 microradians with a resolution of better than 0.2 nanoradians.

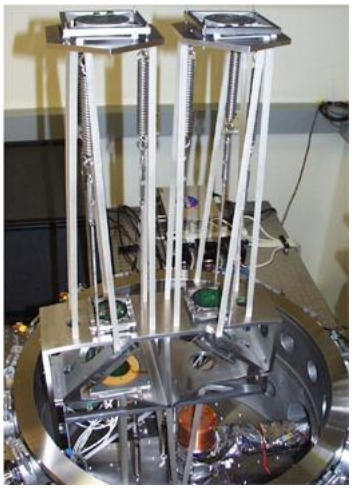

Figure 5. Interferometer design.

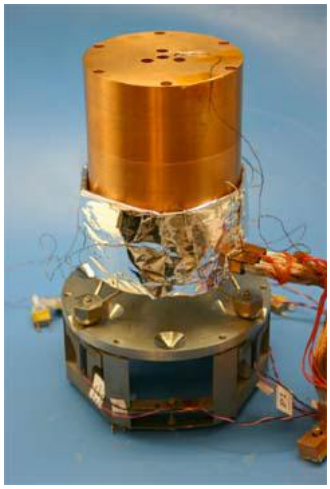

Figure 6. Test sample alignment stage.

2.5 Signal processing electronics data acquisition system

Output from the four photo-detectors and pre-amplifiers of the interferometer pass through noise filters and exit the vacuum chamber via hermetically sealed electrical feed-throughs. Each signal is then processed by its own temperature-controlled post-amplifier electronics which generates a glitch-free, amplified square wave of the proper frequency by means of a zero-crossing detector and phase-locked-loop (PLL). These four square waves are then read and interpreted by a phase meter board to produce measurements of differential movement within the test sample. A PC based LabVIEW software system is used for all data acquisition and control of the cryogenic dilatometer. Interferometer data, temperatures, laser output, heater powers, and sample alignment are all graphically displayed in real time and stored to disk.

2. TEST SAMPLE PREPARATION

The raw PMN material consisted of three sample boules labeled A, B, and C and shown in Figure 7 below. All three boules were provided by John Trauger at JPL and were originally manufactured by Xinetics Inc. Significant time was spent trying to locate a vendor capable of fabricating test samples to the stringent parallelism requirements of the dilatometer (4 arcsec) and also willing to work with a relatively uncommon potentially hazardous lead-based material. Eventually, a vendor was identified (Insync Optics in Albuquerque, NM) and a total of nine test samples were successfully fabricated from the three raw sample boules. Each test sample is approximately 5mm x 5mm with a length of 5 – 10mm depending on its parent boule. One of the manufacturing requirements was that crystal orientation, boule traceability, and original location within the boule be maintained for each test sample. Although the original goal was to machine test samples with two axes of measurement per sample, fabrication limitations required that each test sample have only one axis of measurement (z-axis). Therefore, the basic approach was to polish the top and bottom surface of a boule until the parallelism and surface quality requirements were satisfied. Then the boule was sectioned to extract three test samples from it. Shown below in Figure 8 are the nine PMN test samples fabricated by Insync Optics.

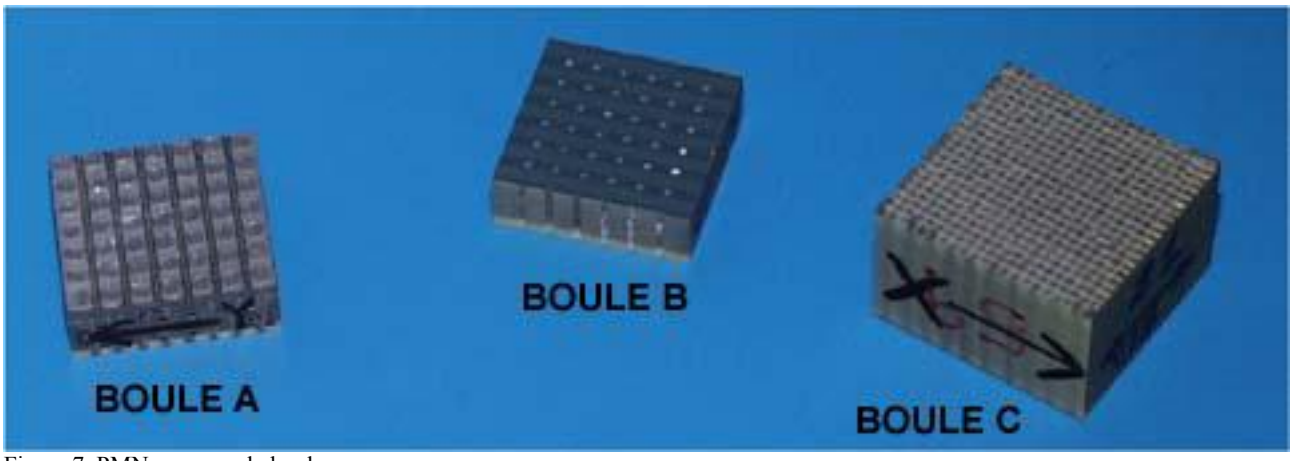

Figure 7. PMN raw sample boules.

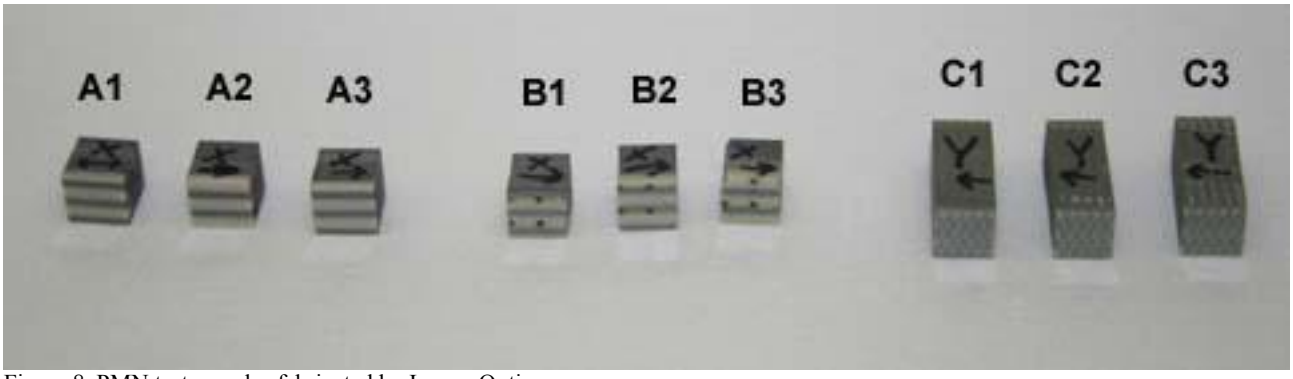

Figure 8. PMN test samples fabricated by Insync Optics

3. TEST METHODOLOGY

The basic test configuration of the PMN samples is shown in Figure 9. A PMN sample is placed in contact with polished single crystal silicon reference flat using a drop of isopropyl alcohol. Three calibrated silicon diode temperature sensors are attached around the diameter of the silicon base using a combination of 3M Y966 pressure sensitive adhesive and kapton tape. Due to the small sample size relative to the size of the temperature sensors, and because the sample was not bonded or optically contacted to the base, no temperature sensors were mounted directly on the sample. The concern was that stress from the sensor mounting and lead wire tension would obscure the thermal strain behavior of the PMN material. Therefore, the assumption was made that the difference in temperature between the PMN sample and the silicon base was small for room temperature measurements with relatively slow heating and cooling rates. This assumption was later verified by examining results at multiple heating/cooling rates.

The thermal expansion measurements were made using the methods typical for this facility. The test sample and reference base are mounted inside a copper shroud that is thermally controlled using two film heaters and a closed-cycle helium refrigerator. An interferometer compares a center light beam reflected off the top of the sample to the average of three outer beams reflected off of the top of the reference base to determined the thermal expansion or contraction of the sample. The entire test is performed in vacuum.

3.1 Data sets

A total of seven data sets were developed for the testing of PMN boules A and C as shown in Table 1.

Table 1. Testing parameters associated with PMN Boules A and C

Data Set	Test Approach	Thermal Profile	Temperature Transitions	Number of Cycles
PMN A1 2005/01/25	Transient	310K to 270K to 310K	1.5 K/hr	2
PMN A1 2005/01/27	Steady State	310K to 270K to 310K at 5 K increments	15 K/hr	1
PMN A1 2005/01/31	Transient	310K to 270K to 310K	1.75 K/hr	1
PMN A2 2005/02/10	Transient	310K to 270K to 310K	1.75 K/hr	1
PMN C1 2005/01/20	Transient	310K to 270K to 310K	3.5 K/hr	2
PMN C2 2005/03/02	Transient	310K to 270K to 310K	8 K/hr	7
PMN C2 2005/03/07	Transient	310K to 270K to 310K	3 K/hr	3

For the purpose of this paper, a transient testing approach is defined as having a nominal thermal profile of 310K to 270K to 310K with setpoints defined as the maximum and minimum temperatures of interest. The steady state temperature testing approach has the same nominal thermal profile; however the temperature is incremented in 5K steps and held until the sample reaches a steady state temperature stability of +/- 5mK.

The results presented in this paper will focus on the data sets developed for PMN C2 2005/03/07 and PMN C2 2005/03/02. Since these data sets undergo a transient testing approach a local CTE was deemed most appropriate in order to minimize errors. The remaining data sets will be used to document the variability between boules A and C.

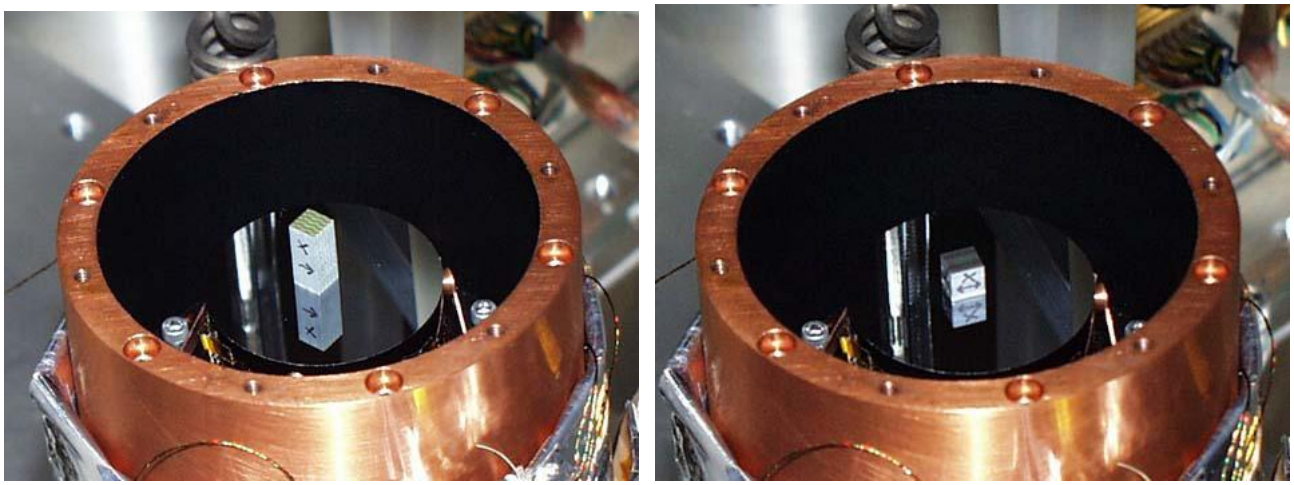

Figure 9. Test samples #C1 (left) and #A1(right) on silicon base inside copper thermal shroud.

4. DATA ANALYSIS

4.1 Local CTE derivation

The local CTE is determined by evaluating the derivative of a least squares nth order polynomial curve fit applied to the raw strain data. It is important to note that curve fitting techniques can produce end effects resulting in larger uncertainties associated with the ends of the data set. Therefore, the order of the curve fit is established by minimizing both nonlinearities and deviations associated with the residuals of the curve fit as well as minimizing end effects. The curve fitting process is highly unsystematic and is largely up to the discretion of the data analyst; however by fallowing the aforementioned requirements user developed errors can be minimized. For the purpose of this analysis, MATLAB's

"polyfit" and "polyder" command were used to develop the necessary equations for both the nth order least squares polynomial curve fit as well as local CTE results respectively.

5. RESULTS & CONCLUSIONS

5.1 Thermal strain and CTE results

Figure 10 shows the raw thermal strain measurements for data sets PMN C2 2005/03/02 and PMN C2 2005/03/07. The raw data suggest that some amount of lag exists between the average sample temperature and the measurement temperature, albeit small, resulting from ramp rates greater than 3K/hr as seen in Figure 11.

It was determined that a least square 3rd order polynomial curve fit best met the requirements specified in Section 4. The resulting thermal strain and CTE curves are shown in Figure 12 and 13 respectively. The results show that the PMN sample contracts by ~61 ppm from 310 K to 270 K. Additionally, the results show that the coefficient of thermal expansion decreases from ~1.61 ppm/K to a value of ~1.51 ppm/K over a temperature range of 310 K to 288 K. The CTE then increases to a value of ~1.57 ppm/K at a temperature of 270 K.

The strain standard deviations are given in Figure 14. The standard deviation of the strain data was computed by calculating the variability of the strain curves at 1 K temperature increments. The plot shows that a maximum standard deviation of ~0.17 ppm occurs at 310 K and decreases to a value of ~0.1 ppm at 290 K and then begins to increases to ~0.16 ppm at 270 K. The larger standard deviation values found at 310 K and 270 K are the result of end effects due to curve fitting, and result in the greater variability of CTE values at 310 K and 270 K.

To investigate variations between boules, Figure 15 shows CTE data for boules A and C. Each boule had three samples cut from it, and these samples' CTE, individually plotted, show that the CTEs of the samples from a given boule are consistent with each other, within the standard deviation values of Figure 14, but that the boules themselves have distinct CTEs. The difference in boule CTEs is presumably due to compositional differences.

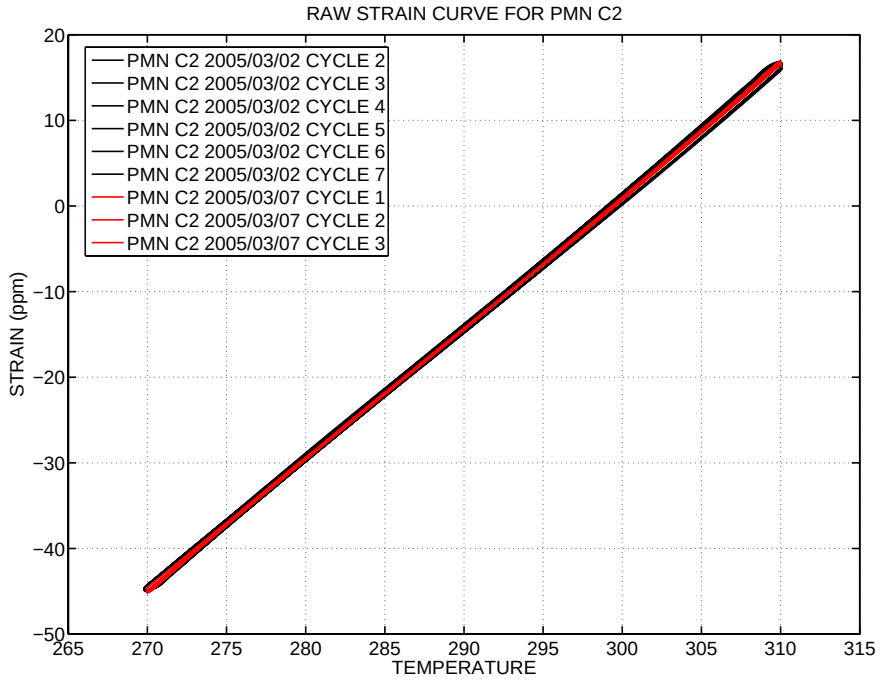

Figure 10. Compiled strain curve of raw data for PMN C2 2005/03/02 and PMN C2 2005/03/07 over a nominal thermal profile of 310K to 270K to 310K.

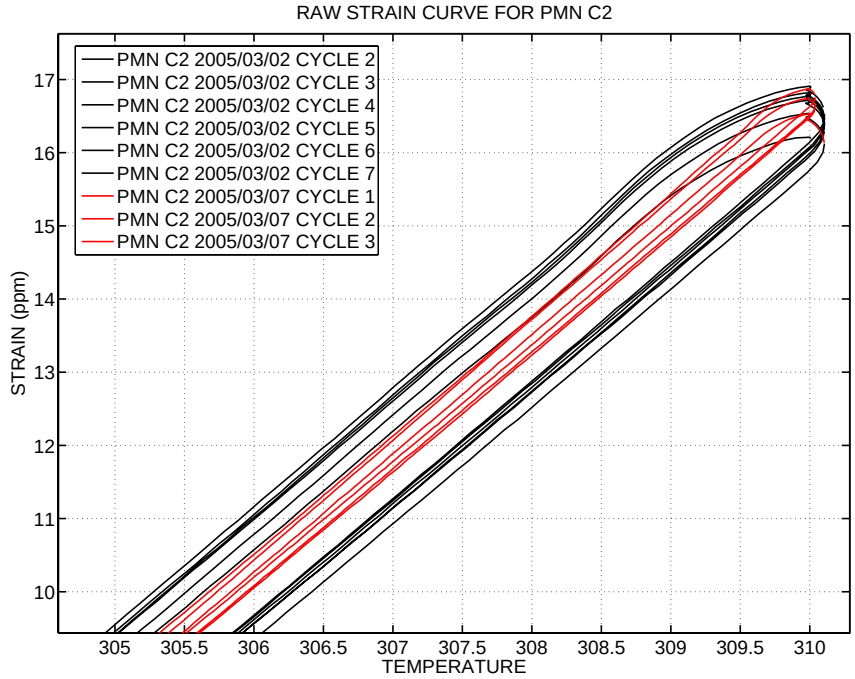

Figure 11. Observed temperature measurement lag of PMN sample C2 with ramp rates greater than 3 K/hr.

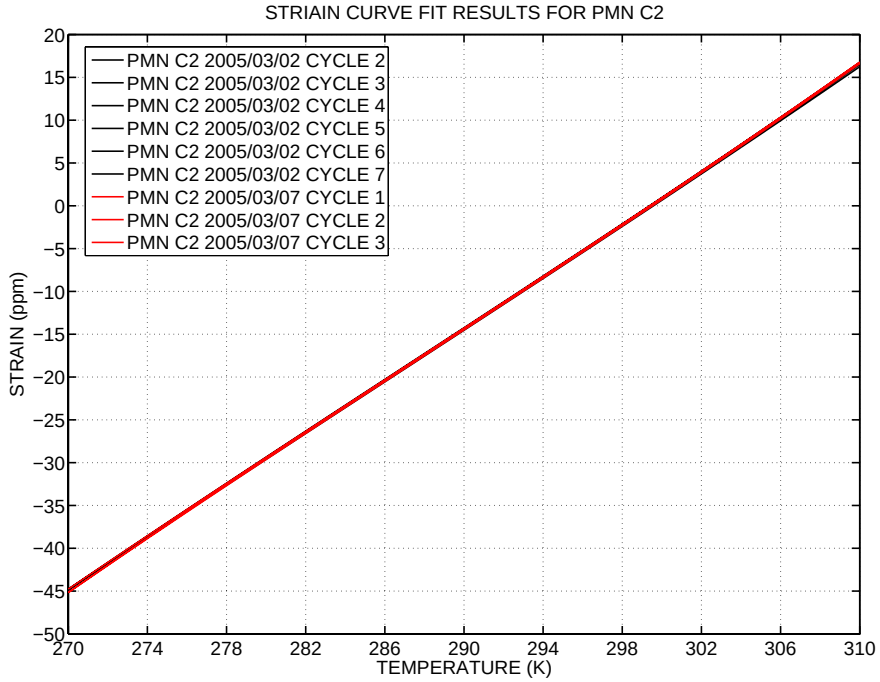

Figure 12. Least square 3rd order polynomial curve fit to each cycle of PMN C2 2005/03/02 and PMN C2 2005/03/07.

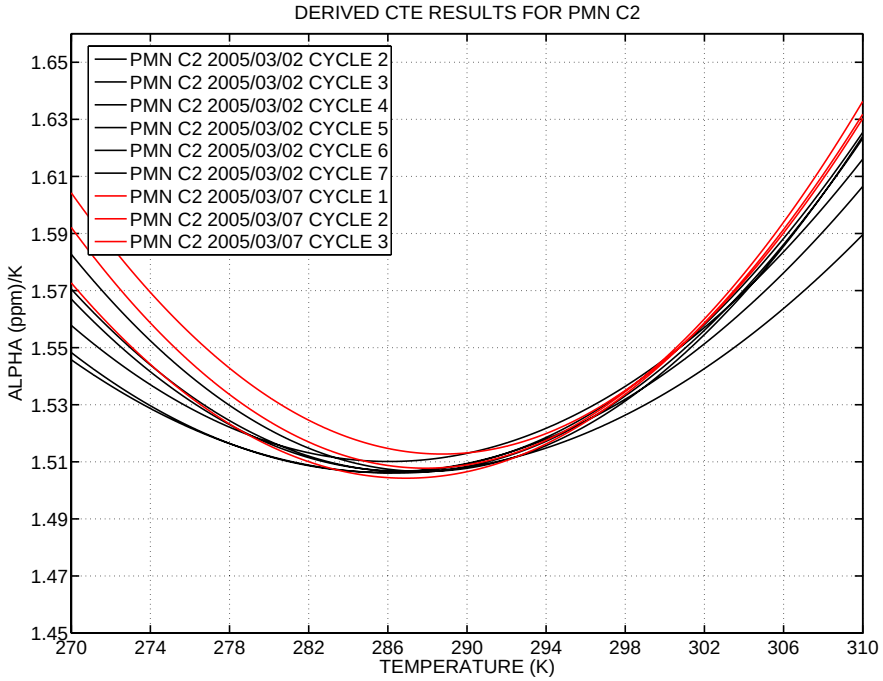

Figure 13. Derived local CTE for PMN C2 2005/03/02 and PMN C2 2005/03/07.

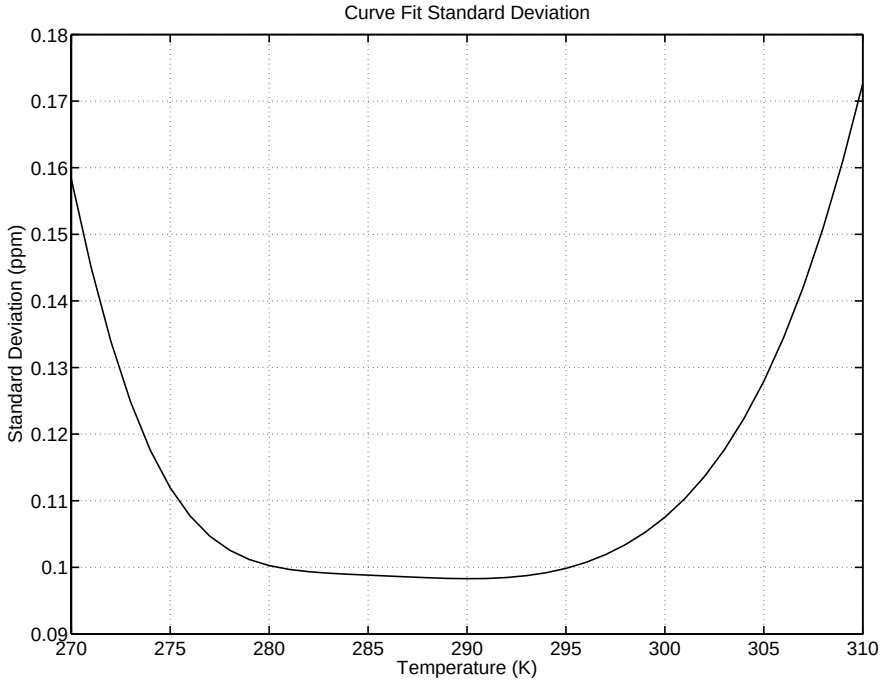

Figure 14. Standard deviations associated with the variability of PMN sample C2 curve fits in 1 K temperature increments.

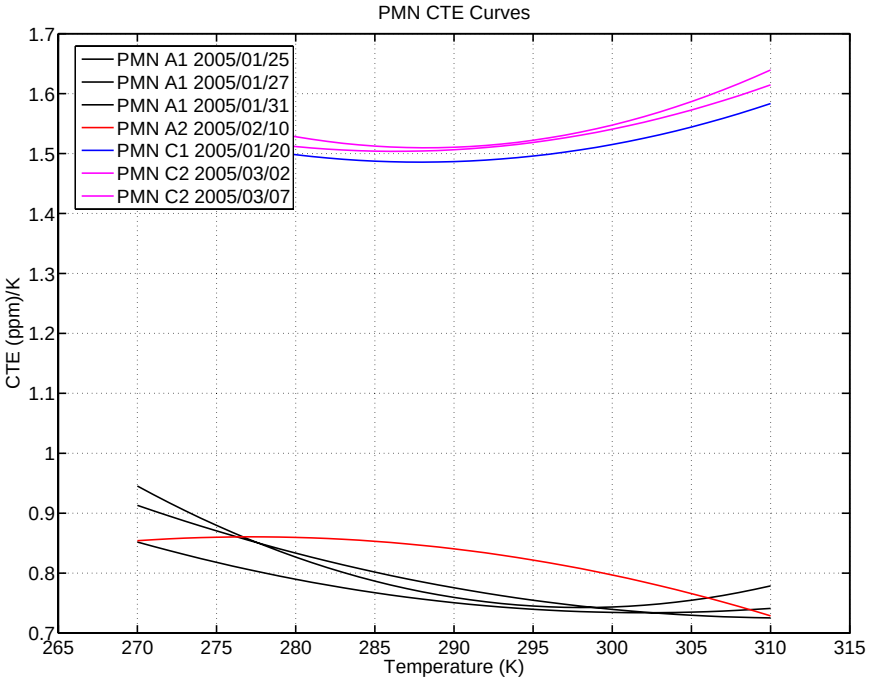

Figure 15. Local CTE for samples taken from boules A and C. CTE difference between A and C is presumed to be caused by a difference in composition.

6. FUTURE PLANS

The PMN material obtained for this study was originally manufactured several years ago. Since then Xinetics has been working to make improvements and alternative formulations of the material to satisfy the demands of their customers. Now that test sample fabrication has been demonstrated, and the ability to measure their CTE has been verified, future plans are to fabricate new test samples from one of the more recent PMN formulations. For these new samples, larger PMN boules will be made available. Therefore, fabrication of larger sample pillars (25.4mm long), measurements in multiple boule axes, and fabrication of PMN sample bases will be possible.

Later this year, the current facility laser source will be replaced by a commercially available, frequency stabilized, laser source. By locking the frequency of the laser to one of the major absorption lines of iodine, this upgrade will eliminate system error due to long-term drift of the laser. Also planned for later this year is a demonstration of the ability to fabricate and test metallic samples such as aluminum, Invar and titanium.

ACKNOWLEDGEMENTS

The authors would like to thank NASA's James Webb Space Telescope, Terrestrial Planet Finder Coronagraph, and Space Interferometry Mission projects for their continuing support for the development of the JPL Cryogenic Dilatometer Facility. Additional thanks go to John Trauger for initially supplying the raw PMN material from Xinetics and to Insync Optics for fabrication of all of the PMN test samples.

This research was carried out at the Jet Propulsion Laboratory, California Institute of Technology, under a contract with the National Aeronautics and Space Administration.

REFERENCES

1. M. Dudik, P. Halverson, M. Levine, M. Marcin, R. Peters, S. Shaklan, "Development of a Precision Cryogenic Dilatometer for the James Webb Space Telescope Materials Testing," *SPIE Proceedings of Optical Materials and Structures Technologies,* **vol. 5179**, p. 155-164, 2003.
2. P. Karlmann, M. Dudik, P. Halverson, M. Levine, M. Marcin, R. Peters, S. Shaklan, D. Van Buren, "Continued development of a precision cryogenic dilatometer for the James Webb Space Telescope," *SPIE Proceedings of Space Systems Engineering and Optical Alignment Mechanisms*, **vol. 5528**, p. 63-71, 2004.
3. F. Zhao, J. Logan, S. Shaklan, M. Shao, *SPIE Proceedings of Optical Engineering for Sensing and Nanotechnology*, **vol. 3740**, p. 642, 1999.
4. F. Zhao, *Proceedings of the ASPE Annual Meeting*, p. 345, 2001.

* paul.b.karlmann@jpl.nasa.gov; phone (818) 354-7876; fax (818) 393-4206